Static and dynamic properties of helical spin chains

de Raedt, Hans; Raedt, Bart De

Published in:
Physical Review B

DOI:
10.1103/PhysRevB.19.2595

Publication date:
1979

PHYSICAL REVIEW B VOLUME 19, NUMBER 5 1 MARCH 1979

Static and dynamic properties of helical spin chains

Hans De Raedt
Departement Natuurkunde, Universitaire Instelling Antwerpen, B-2610 Wilrijk, Belgium

Bart De Raedt
Institut für Theoretische Physik, Universität des Saarlandes, D-6600 Saarbrücken, Germany
(Received 25 September 1978)

A detailed quantitative study of a classical Heisenberg chain with nearest- and next-nearest-neighbor interaction is presented. For a wide range of interaction strength, this model leads to helical structures and the effects of this peculiar structure on the static and dynamic properties is extensively discussed. The most striking feature is the presence of both a central resonance and a spin-wave peak at fairly low temperatures.

I. INTRODUCTION

In this paper, we calculate the static and dynamic properties of a one-dimensional Heisenberg model with nearest- and next-nearest-neighbor interaction. For certain values of the ratio of the nearest- and next-nearest-neighbor interaction, this model leads to helical spin structures at zero temperature. An interesting feature of this model is that it exhibits a Lifschitz point,[1] i.e., a triple point for the paramagmentic, ferromagnetic, and helimagnetic phases at $T=0$; but it is beyond the scope of this work to examine this particular problem.

Although the helical order disappears for $T \neq 0$,[2] helical short-range order will be present at low temperatures. To our knowledge, it is not known how this peculiar structure affects the dynamical behavior of the system and therefore it is our main purpose to elucidate the differences between this model and the nearest-neighbor chain. Since there is little information about the static properties as well, extensive results for both static and dynamic quantities will be presented.

By transforming the spin-$\frac{1}{2}$ model into a fermion model, Niemeijer calculated the ground-state properties in the Hartree-Fock approximation.[3] Since a calculation of temperature-dependent static quantities would already require an enormous computational effort, the assumption that the essential behavior of the system remains the same when the spin operators are replaced by classical vectors will enable us to calculate all relevant temperature-dependent static properties numerically.

Since it will be very difficult to find exact solutions of the equations of motion, it is necessary to use either numerical techniques or approximative analytic methods. As for the nearest-neighbor chain, the most direct way to study the model would involve a "molecular-dynamics" calculation.[4] Since computer time is finite, these simulations suffer from a severe limitation. Indeed, a detailed quantitative study is only possible if a fast algorithm for generating equilibrium configurations is available.[5] Then, averages over different configurations can be calculated efficiently. Furthermore, it should be noted that, even for the nearest-neighbor chain, a considerable amount of fitting procedures are necessary before numerical estimates for the frequency and damping of the collective excitations are obtained.[6]

As it would not be hard to convince oneself that, because of the next-nearest-neighbor interaction, such an algorithm does not exist, we are led to the conclusion that it is more appropriate to use analytic methods. As in our preceding papers,[7,8] we will use a method based on Mori's formalism.[9] In this way a continued-fraction representation for the dynamical structure factor is obtained directly. For practical purposes, one has to make an approximation for the memory function and, as outlined in Ref. 7, this can be done in a consistent, systematic way without introducing phenomenological relaxation rates. As the final result for the dynamical structure factor is formally the same as for the nearest-neighbor chain, a direct comparison between the two models is possible.

In Sec. II, we discuss some elementary ground-state properties of the model and we derive the dispersion relation. The results for the static correlation functions for different temperatures and wave vectors are presented in Sec. III. We argue that the temperature and wave-vector dependence of these correlation functions can be related to the particular shape of the dispersion relation. In Sec. IV, the

dynamical form factor is calculated. The differences between the line shapes of this model and those of the nearest-neighbor chain are interpreted in terms of the respective dispersion relations. The conclusions are summarized in Sec. V.

II. MODEL AND GROUND-STATE PROPERTIES

The model consists of a chain of classical spins of unit length, placed at unit distance from each other. The Hamiltonian is given by

$$H = -J_1 \sum_i \vec{S}_i \cdot \vec{S}_{i+1} - J_2 \sum_i \vec{S}_i \cdot \vec{S}_{i+2} . \tag{2.1}$$

We now investigate the zero-temperature properties of this model in the case $J_1 > 0$ and $J_2 < 0$.

The ground-state energy is found by minimizing the Hamiltonian, given by Eq. (2.1). For $|J_2| < \frac{1}{4} J_1$, the spins are ordered ferromagnetically at zero temperature. For $|J_2| > \frac{1}{4} J_1$ the ground state is a helix. In this case, all the spins lie in parallel planes, and there is an angle ψ between each spin and its nearest neighbor on one side. It should be noted that the ground state is degenerate, because the plane can be chosen arbitrarily. The angle ψ is determined by the relation

$$\cos\psi = J_1/4\,|J_2|, \quad |J_2| \geq \tfrac{1}{4} J_1 . \tag{2.2}$$

In the following, we will always consider the case $|J_2| \geq \frac{1}{4} J_1$.

Because the system has translational invariance we perform a Fourier transform,

$$\vec{S}_k = \frac{1}{N^{1/2}} \sum_n \vec{S}_n e^{ikn} , \tag{2.3}$$

and then the Hamiltonian reads

$$H = -\tfrac{1}{2} \sum_k J(k) \vec{S}_k \cdot \vec{S}_{-k}, \tag{2.4}$$

with

$$J(k) = 2J_1 \cos k + 2J_2 \cos(2k) . \tag{2.5}$$

The two-spin correlation function in the ground state is simply

$$\langle \vec{S}_i \cdot \vec{S}_{i+n} \rangle_{T=0} = \cos(n\psi) , \tag{2.6}$$

and consequently the Fourier-transformed correlation function reads

$$\langle \vec{S}_{-k} \cdot \vec{S}_k \rangle_{T=0} = \tfrac{1}{2}[\delta(k-\psi) + \delta(k+\psi)] . \tag{2.7}$$

For a classical system the static susceptibility is defined by[10]

$$(\vec{S}, \vec{S})_k = \beta \langle \vec{S}_{-k} \cdot \vec{S}_k \rangle , \tag{2.8}$$

where β is the inverse temperature, and in the ground state we find

$$(\vec{S}, \vec{S})_k = 2/[J(\psi) - J(k)], \quad T = 0 . \tag{2.9}$$

$\vec{S}_{k=\psi}$ is the critical variable, because the static susceptibility diverges at $k = \psi$.

At zero temperature, excitations will propagate undamped along the spin chain. The time-dependent correlation function is then given by

$$\langle \vec{S}_{-k}(t) \cdot \vec{S}_k(0) \rangle_{T=0} = \langle \vec{S}_{-k} \cdot \vec{S}_k \rangle_{T=0} \cos[\Omega(k) t] \tag{2.10}$$

and the dispersion relation $\Omega(k)$ is found to be

$$\Omega(k) = \{\tfrac{1}{2}[J(\psi) - J(k)] \times [2J(\psi) - J(\psi - k) - J(\psi + k)]\}^{1/2} . \tag{2.11}$$

Consequently, the dynamical structure factor consists of two δ functions, symmetric with respect to the origin, and with their positions determined by $\Omega(k)$, i.e.,

$$S(k, \omega)_{T=0} = \langle \vec{S}_{-k} \cdot \vec{S}_k \rangle_{T=0} \times \tfrac{1}{2}[\delta(\omega - \Omega(k)) + \delta(\omega + \Omega(k))] . \tag{2.12}$$

The dispersion-relation equation (2.11) is plotted in Fig. 1 for $\psi = \frac{1}{4}\pi$ and $\psi = \frac{1}{3}\pi$, for the ferromagnet

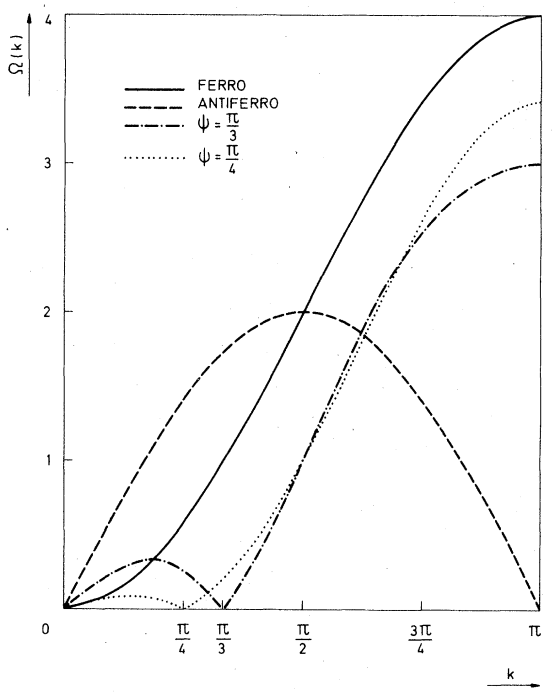

FIG. 1. Dispersion relations for the nearest-neighbor ferro- and antiferromagnet, and for the helical chain for the angles $\psi = \frac{1}{3}\pi$ and $\psi = \frac{1}{4}\pi$.

($J_1 > 0$, $J_2 = 0$), and for the antiferromagnet ($J_1 < 0$, $J_2 = 0$). In all cases the excitation energy is zero for zero wave vector. This is a consequence of the total spin being a conserved quantity. The other point in the Brillouin zone where the excitation energy is zero, is determined by the critical wave vector.

Although the results, presented above, only hold in the ground state, they tell us what we can expect for the low-temperature behavior of the system. It is well known that no long-range order exists in one-dimensional systems with finite range interactions at nonzero temperatures.[2] At low temperatures however, there exists a strongly developed short-range order, characterized by a correlation length ξ. It is not so easy to give a definition for the correlation length for a helimagnet as for a ferro- or antiferromagnet. A plausible definition is as follows. At low temperatures the static correlation function [see Eq. (2.7)] consists of two peaks, symmetric with respect to the origin of the Brillouin zone. The correlation length is defined as the inverse of the width of such a peak. The spins within a segment of the chain with a length shorter than the correlation length will be strongly correlated. The correlation over distances much larger than the correlation length however, will be small.

In Secs. III and IV, we will deal with the ferromagnetic case $J_1 > 0$ only, and we will put $J_1 = 1$. Clearly, this is no limitation, since it means that we measure J_2, and the temperature, in units of J_1.

III. STATIC CORRELATION FUNCTIONS

If we want to calculate the temperature-dependent static spin-spin correlation function for different values of ψ, there is little hope to find analytic expressions because the problem of evaluating the partition function is obviously very difficult. Furthermore, the static quantities that will show up in our dynamical description, are very complicated combinations of spin correlation functions. Consequently, it is desirable to use a numerical method that has sufficient accuracy, is relatively easy to program and requires a modest effort of human work.

In an earlier paper,[8] we have shown that the Monte Carlo method has all the desired features. For a description of the Monte Carlo method for spin systems, we refer the interested reader to the paper of Binder.[11] For all our calculations, we have taken a chain of 250 spins, 2000 Monte Carlo steps per spin were used to eliminate the effect of the initial configuration, and the thermodynamic quantities were calculated by averaging over 400 different spin configurations in a Monte Carlo run of 4000 steps per spin. In order to calculate the statistical errors, 12 statistically independent runs were averaged and by calculating the variance, we concluded that the absolute error on the correlation functions is smaller than 10^{-2}.

To examine the influence of the starting configuration the ground state was taken as the initial configuration for six runs, while a random configuration was used for the remaining six runs. The similarity between the results for both cases is an important measure for the accuracy of the method, and for extremely low temperatures large differences appear. This is readily understood because it is well known that the statistical errors grow rapidly if one approaches the critical temperature $T = 0$.[11] This, however, is not the case for the results presented in this paper. Let us now look at the data for the static correlation functions $\langle \vec{S}_0 \cdot \vec{S}_n \rangle$, $n = 0, 1, \ldots, 20$ for different temperatures and angles ψ (see Figs. 2–4). As expected, the correlation becomes stronger as the temperature decreases. For larger distances (i.e., $n > 4$) the chosen angle ψ is clearly reflected in the periodicity of the correlation function.

Comparing correlation functions for different angles but for the same temperature, we note that the correlation increases as the angle increases or in other words, the larger the angle ψ, the more stable the helical structure is. This can be explained by considering the shape of the dispersion relation (Fig. 1) which is a measure for the distribution of the energy. At very low temperature, the ground state $k = \psi$ and a few excited states are accessible. Since the slope of the dispersion relation at $k = \psi$ increases if ψ increases, the density of states, which is proportional to the inverse of the slope decreases, and therefore, the number of accessible states at sufficiently low temperature is smaller for large angles than for small angles. This simple argument explains why a helix with a larger angle is more stable than a helix with a smaller angle if the temperature for both helices is the same. Although the correlation functions shown in Figs. 2–4 have some interesting features, the quantity of more fundamental interest is the Fourier-transformed static correlation function

$$\langle \vec{S}_{-q} \cdot \vec{S}_q \rangle = 1 + 2 \cdot \sum_{n=1}^{M} \langle \vec{S}_0 \cdot \vec{S}_n \rangle \cos(qn) \ . \qquad (3.1)$$

In theory, M should be equal to N but in actual calculations we have taken $M = 50$.

A typical plot of $\langle \vec{S}_{-q} \cdot \vec{S}_q \rangle$ for different temperatures and $\psi = \frac{1}{4}\pi$ is shown in Fig. 5. As the temperature increases, the contribution of the critical wave vector $q = \psi$, decreases. Clearly, the Fourier-transformed correlation function is asymmetric around $q = \psi$. This is entirely due to the shape of the dispersion relation Fig. 1, because excitations with wave vector left to $q = \psi$ have lower energy than excitations with a corresponding wave vector right to $q = \psi$, and consequently their probability of being occupied is larger. As the figures for the Fourier-

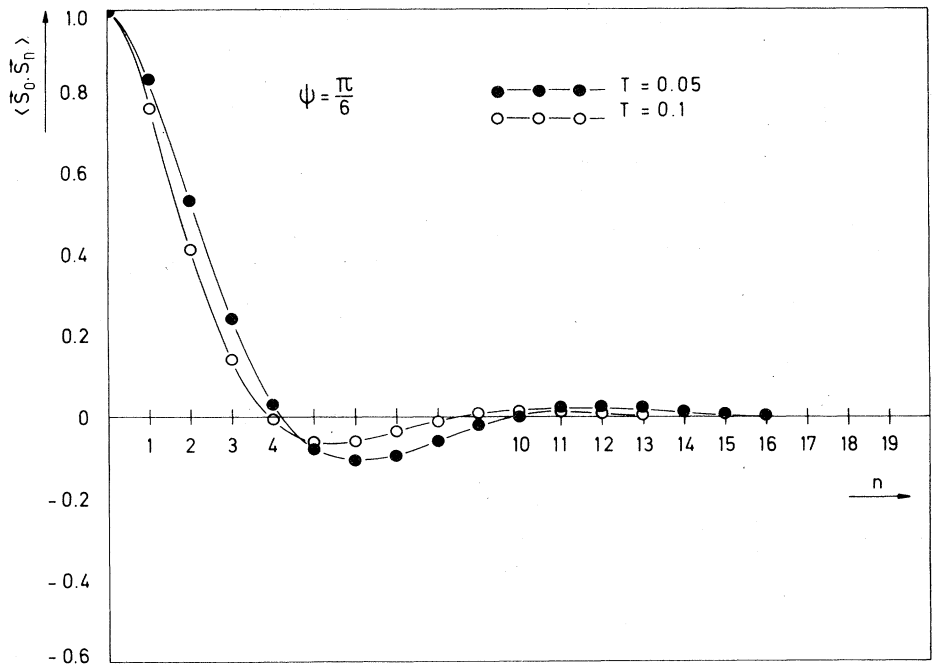

FIG. 2. Spin-spin correlation function as a function of the distance and the temperature. At $T=0$, the angle between nearest-neighbor spins is $\psi = \frac{1}{6}\pi$. The solid lines are guides for the eye only.

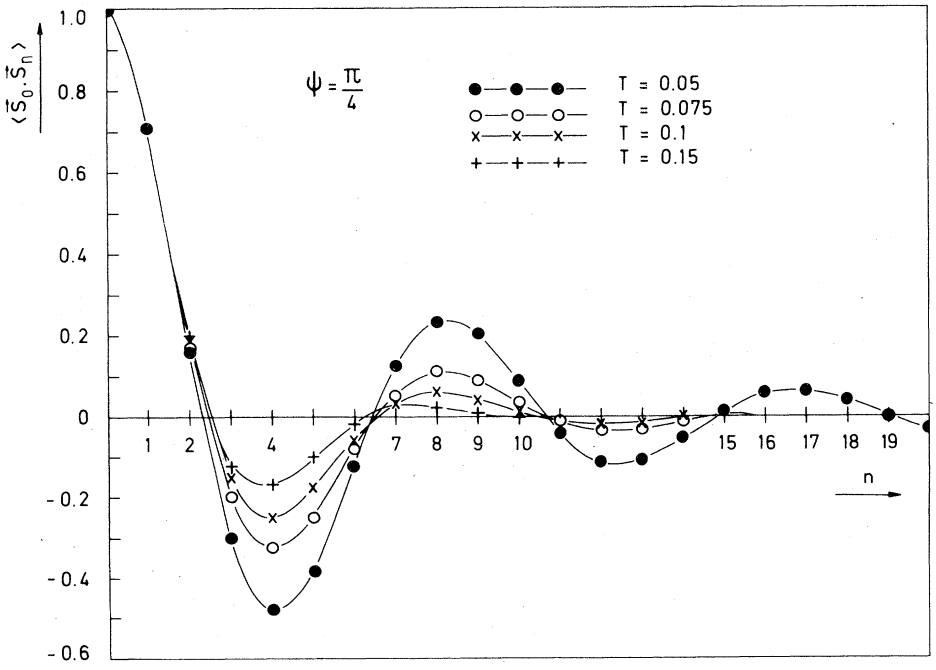

FIG. 3. Same as Fig. 2 but $\psi = \frac{1}{4}\pi$.

transformed correlation functions for $\psi=\frac{1}{3}\pi$ and $\psi=\frac{1}{6}\pi$ are very similar, they have not been presented.

IV. DYNAMIC CORRELATION FUNCTIONS

Having discussed the zero-temperature properties and the behavior of $\langle \vec{S}_q \cdot \vec{S}_{-q} \rangle$ as a function of ψ, q, and T, we now want to study the low lying collective excitations of our model system. In our opinion, the most appropriate way to do this is to use Mori's formalism.[9] The Laplace-transformed relaxation function is written as a continued fraction and the coefficients appearing in these expansions are related to the frequency moments of the relaxation function.

The only unknown quantity is the memory function and we will use the method, extensively discussed in our earlier papers,[7,8] to determine this function. As the calculation is identical to the one given in Ref. 7, we do not want to repeat it here, but only stress the facts that in our approach, no phenomenological parameters have to be introduced and all possible sum rules are exactly fulfilled. The final result for the normalized Laplace-transformed relaxation function is

$$\Phi_{ss}(z,q)=\frac{z^2+z\,\Sigma(z,q)-\langle\omega^4\rangle_q/\langle\omega^2\rangle_q+\langle\omega^2\rangle_q}{z(z^2-\langle\omega^4\rangle_q/\langle\omega^2\rangle_q)+\Sigma(z,q)(z^2-\langle\omega^2\rangle_q)}\,,\quad z=\omega+i\epsilon\,,\quad \epsilon>0\,, \tag{4.1}$$

while the expression for the memory function reads

$$\Sigma(z,q)=-\frac{(\langle\omega^6\rangle_q-\langle\omega^4\rangle_q^2/\langle\omega^2\rangle_q)/(\langle\omega^4\rangle_q-\langle\omega^2\rangle_q^2)}{z+i[(\langle\omega^6\rangle_q-2\langle\omega^4\rangle_q\langle\omega^2\rangle_q+\langle\omega^2\rangle_q^3)/(\langle\omega^4\rangle_q-\langle\omega^2\rangle_q^2)]^{1/2}}\,. \tag{4.2}$$

As usual, $\langle\omega^2\rangle_q$, $\langle\omega^4\rangle_q$, and $\langle\omega^6\rangle_q$ denote the second, fourth, and sixth frequency moment of the relaxation function Φ. It is easy to express the second moment

$$\langle\omega^2\rangle_q=4[(1-\cos q)\,\langle\vec{S}_i\cdot\vec{S}_{i+1}\rangle-|J_2|(1-\cos 2q)\,\langle\vec{S}_i\cdot\vec{S}_{i+2}\rangle]/\beta\langle\vec{S}_q\cdot\vec{S}_{-q}\rangle\,, \tag{4.3}$$

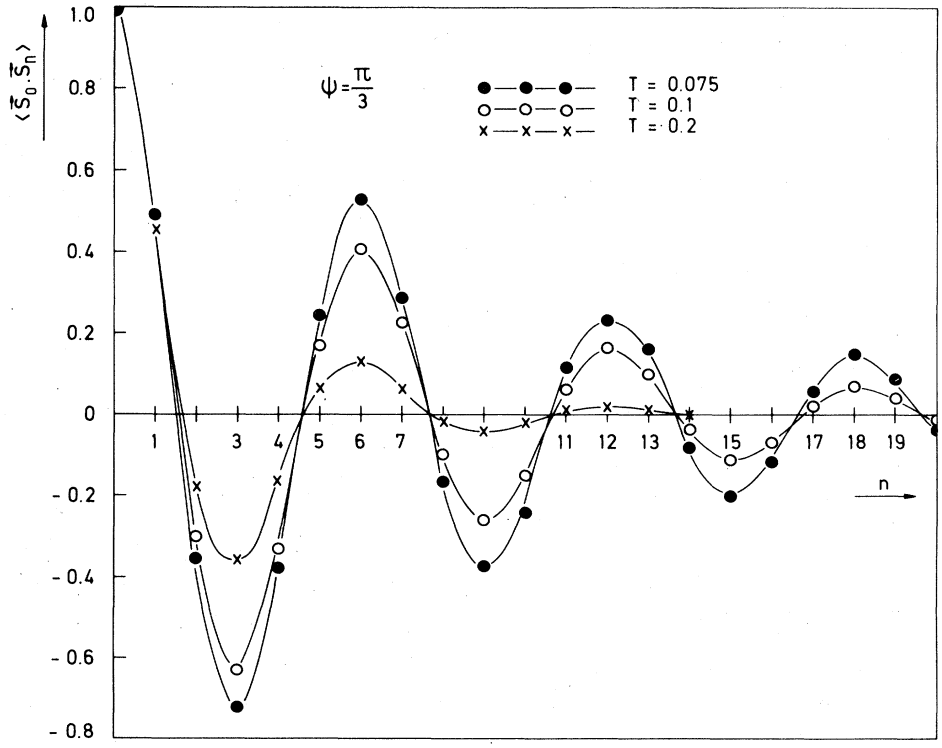

FIG. 4. Same as Fig. 2 but $\psi=\frac{1}{3}\pi$. Note the increasing correlation between the spins if ψ increases.

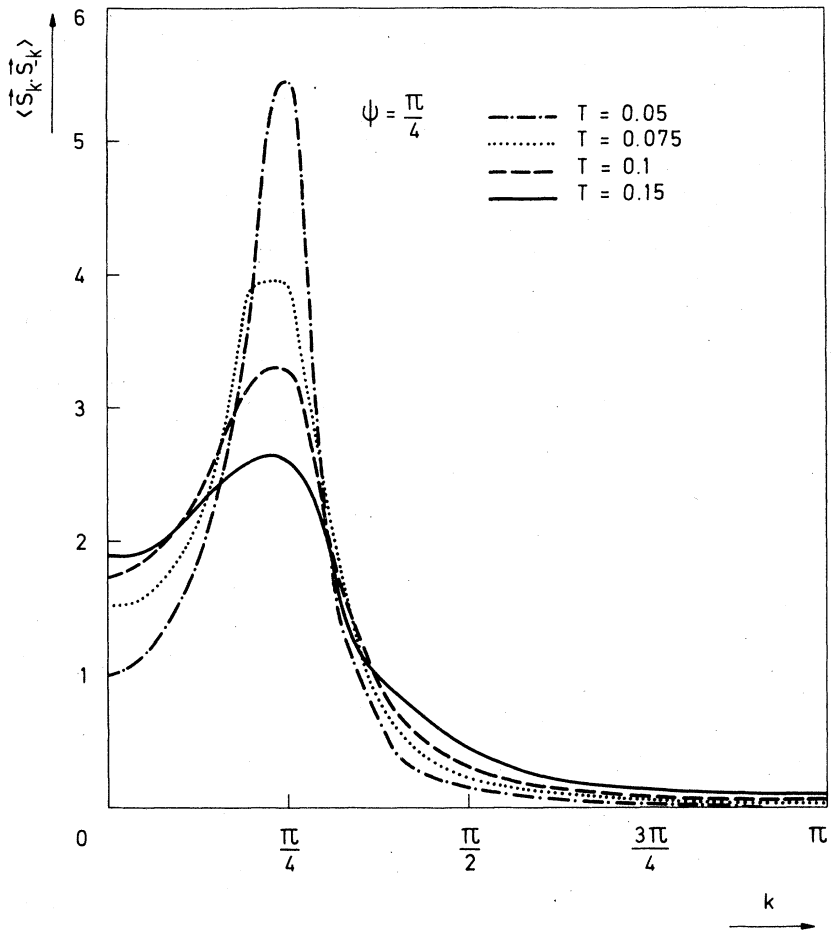

FIG. 5. Typical plot of the Fourier-transformed correlation functions for different temperatures. The angle $\psi = \frac{1}{4}\pi$ is clearly reflected by the maximum at $q = \psi$.

in terms of static two-spin correlation functions, but, if we would like to have similar expressions for the fourth, and sixth moments, the work involved would probably exceed a human life time. Since it is relatively easy to implement a calculation of these moments in a Monte Carlo program, direct numerical results are obtained. As the numerical data itself are not relevant for our discussions, it is unnecessary to present them. Bare results for similar calculations for the planar chain can be found in Ref. 8. Using these numerical values for the moments, the imaginary part of the relaxation function Eq. (4.1), which is proportional to the dynamical form factor for inelastic scattering, i.e.,

$$S(\omega,q) = -\langle \vec{S}_q \cdot \vec{S}_{-q} \rangle \Phi_{ss}''(q,\omega) \tag{4.4}$$

is plotted for several values of ψ, T, and q as a function of the frequency ω.

Let us first consider those wave vectors for which $q \geq \psi$. From Figs. 6–8, we conclude that excitations with wave vectors close to the critical wave vector, are represented by a sharp and very high central peak. This could be expected because the critical modes have low energy. For larger wave vectors, the amplitude of the central peak decreases while the linewidth becomes larger. For q closer to 2ψ excitations with nonzero energy (i.e., spin waves) are visible, and in approaching the Brillouin-zone boundary, the weight of these excitations gets larger and finally the central peak vanishes completely. The presence of both a spin wave and a central peak is astonishing because the temperatures we are considering are very low. We also want to point out that this effect is not due to the particular choice of our relaxation function since it is a four-pole expansion.

Comparing these results with the ones obtained

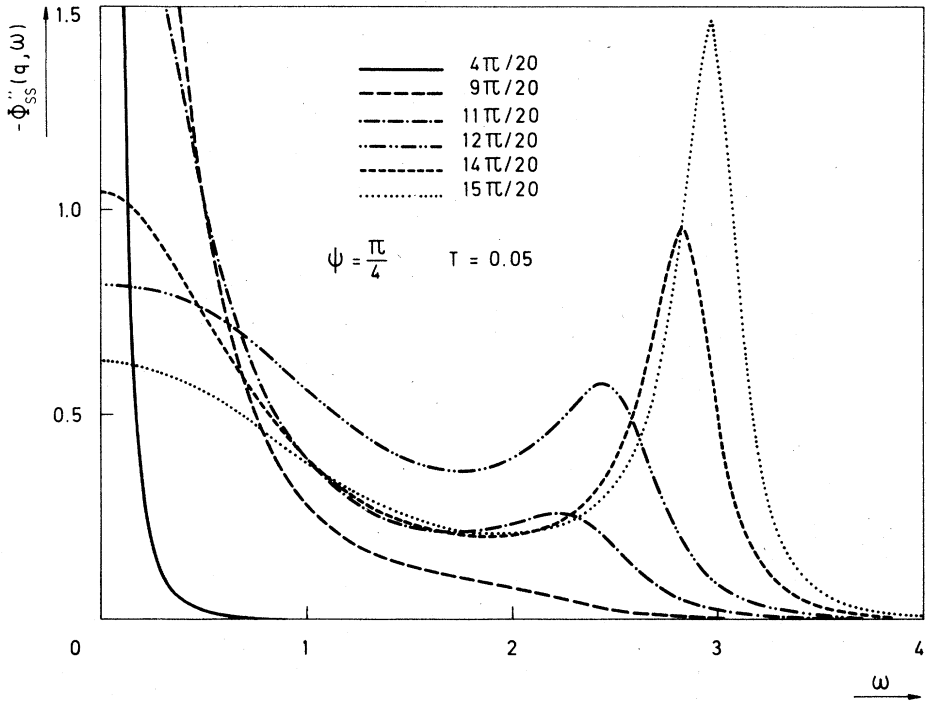

FIG. 6. Normalized dynamical structure factors for $\psi = \frac{1}{4}\pi$ and $T = 0.05$. Note the rapid change in relative intensity of the spin-wave peak for $2\psi < q \rightarrow \pi$.

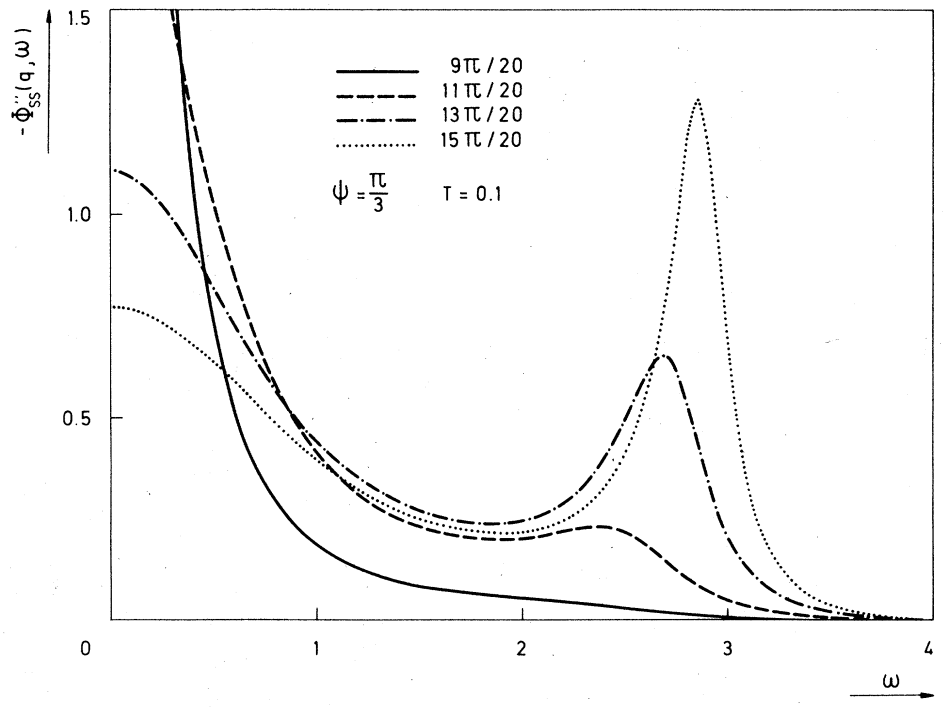

FIG. 7. Normalized dynamical structure factors for $\psi = \frac{1}{3}\pi$ and $T = 0.1$. The fact that a spin-wave peak is visible for $q = \frac{1}{20}11\pi$ is due to the fact that the helix is more stable (compare Fig. 3 and Fig. 4).

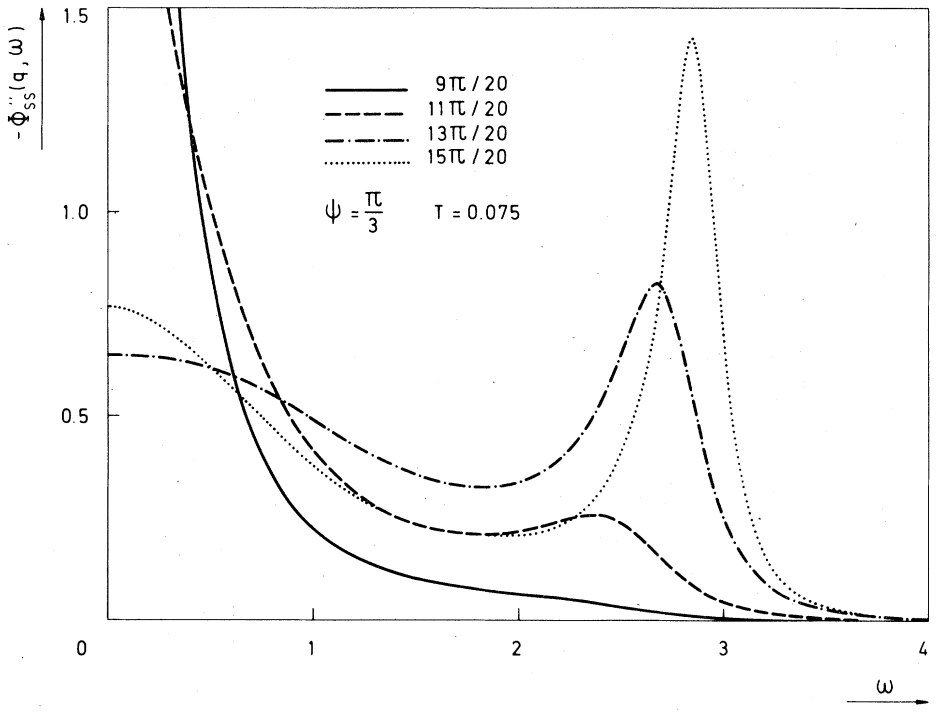

FIG. 8. Normalized dynamical structure factors for $\psi = \frac{1}{3}\pi$ and $T = 0.075$. Compare the contribution of the central peak for $q = \frac{1}{20}13\pi$ with the one of Fig. 7.

from a three-pole expansion, we concluded that the three-pole expansion strongly suppresses spin waves.

In Ref. 7, we showed that this is also the case for the nearest-neighbor chain, but at low temperatures there was no indication of both a central resoance and a spin-wave peak,[6] whereas for this helical model both peaks are observed.

Since Eq. (4.1) shows two peaks at positive energy for the three-dimensional electron gas,[12] we looked for a similar line shape but we did not succeed. Therefore, we believe that Eq. (4.1) approximatively accounts for the real physical phenomena in the system. For $\psi = \frac{1}{3}\pi$, we have also examined the temperature dependence of the line shapes (see Figs. 7 and 8). The most striking feature is the rapid change in the contribution of the central peak relative to the spin-wave contribution at $q = \frac{1}{20}13\pi \approx 2\psi$. These statements, illustrated by means of the few figures presented, are supported by a lot of numerical evidence.

Comparing relaxation functions for the helix and the ferro- or antiferromagnetic nearest-neighbor Heisenberg model, and bearing in mind that in the latter models, there is no evidence for the presence of both a central peak and a spin wave at sufficient low temperature,[6,7] an explanation for these phenomena should be sought in the essentially different shape of the dispersion relation for the helical model.

First, we note that, for each value of q and T, the imaginary part of the relaxation function gives us the probability to find an excitation with energy ω. Then, we recall the fact that the probability for the existence of elementary excitations with wave vector q, i.e., spin waves, is given by the static correlation function. Looking at Fig. 5, it is clear that a spin wave with wave vector smaller than ψ is more likely to exist than a spin wave with the corresponding wave vector larger than ψ.

Now, we fix the temperature and we wonder whether an excitation with wave vector q, consists of one or two spin waves. Obviously, this depends on the probability for these processes. Suppose that the two spin-wave process is more probable. If one of these spin waves has a low energy, it can make a considerable contribution to the zero-frequency behavior, providing the wave vector is close to the critical wave vector. If q is smaller but almost equal to 2ψ, the probability for the existence of a single spin wave is relatively small (for example, see Fig. 5 for $T = 0.05$). It is obvious that the probability for the occurence of two waves of which one spin wave has a wave vector close or equal to ψ, and the other

one has a wave vector $q-\psi$, is much larger. The probability for observing two spin waves reaches a maximum at $q=2\psi$. For $q>2\psi$ it is clear that the probability for a two-spin process vanishes rapidly as q approaches the Brillouin-zone boundary. Applying the same arguments to the ferromagnetic and antiferromagnet, we find that two spin-wave processes are insignificant at low temperatures. We conclude that the picture of competing one and two spin-waves processes gives a consistent qualitative explanation for the simultaneous occurrence of a central peak and a spin wave. Although in our calculations higher order spin-wave processes have been taken into account, the main features can be understood in terms of one and two spin waves because the temperature is very low.

For wave vectors smaller than ψ $(0\leq q\leq\psi)$, our calculations lead us to the following conclusions. Although the probability for elementary excitations is large, we do not observe spin waves if the excitation energy is smaller than the thermal energy, because then the spin waves are overdamped. Since this the case for $\psi=\frac{1}{4}\pi$, $T=0.05$, and $0\leq q\leq\psi$, we did not present these figures because they only show a central peak. For $\psi=\frac{1}{3}\pi$, however, only a limited number of spin waves is thermally excited and the results for different wave vectors and temperatures are given in Fig. 9. For small wave vectors $(\frac{1}{2}q<\psi)$, the spin waves are clearly present if the excitation energy is larger than the thermal energy but the damping is rather large. As expected, no three-peak structure is observed for larger wave vectors. Finally, we note that the renormalization of the excitation energy as a function of the temperature is small in all cases where spin waves are present. At higher temperatures this renormalization becomes more important.

V. CONCLUSIONS

We have calculated the static and dynamical properties of a complicated classical spin chain, exhibiting helical short-range order. Since we were unable to calculate the partition function analytically, we used Monte Carlo techniques. In this way, all relevant static quantities were obtained. We showed that the helical structure is easily recognized by looking at the spatial spin-spin correlation function. At sufficiently low temperatures, the behavior of the static quantities can be understood in terms of the zero-temperature dispersion relation.

As it was our aim to compare the dynamical pro-

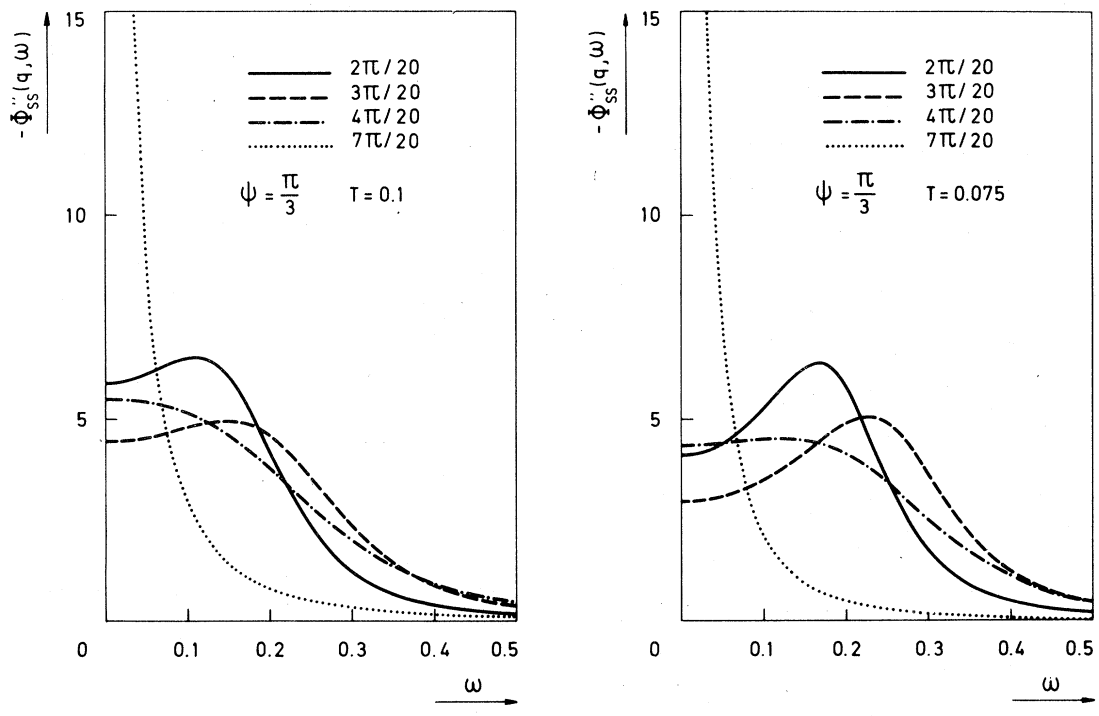

FIG. 9. Normalized dynamical structure factors for $q<2\psi$. The spin waves are stongly damped because of higher-order spin-wave processes.

perties of a helical magnet and a ferromagnet, we used the same description for the dynamics. We find that the helical magnet exhibits a completely different behavior. At fairly low temperatures, both a central peak and a spin-wave peak are found, whereas in the case of the ferro- or antiferromagnet, there is no evidence for the simultaneous occurrence of both peaks.[6,7] This difference has been explained by means of one and two spin waves and the shape of the dispersion relation.

In our opinion, the methods used in this paper could be useful if one likes to study the static and dynamical behavior of the model if one approaches the Lifschitz point $T \to 0$, $\psi \to 0$.

ACKNOWLEDGMENTS

We thank K. H. Michel and W. Selke for useful discussions, for financial support of the project "Neutron Scattering," Interuniversitair Instituut voor Kernwetenschappen is gratefully acknowledged.

[1]W. Selke, Z. Phys. B 27, 81 (1977).
[2]N. D. Mermin and H. Wagner, Phys. Rev. Lett. 17, 1133 (1966).
[3]TH. Niemeijer, J. Math. Phys. 12, 1487 (1971).
[4]M. Steiner, J. Villain, and C. G. Windsor, Adv. Phys. 25, 87 (1976).
[5]N. A. Lurie, D. L. Huber, and M. Blume, Phys. Rev. B 9, 2171 (1974).
[6]P. Heller and M. Blume, Phys. Rev. Lett. 39, 962 (1977).
[7]H. De Raedt and B. De Raedt, Phys. Rev. B 15, 5379 (1977).
[8]B. De Raedt and H. De Raedt, Phys. Rev. B 17, 4344 (1978).
[9]H. Mori, Prog. Theor. Phys. 34, 399 (1965).
[10]R. Kubo, J. Phys. Soc. Jpn. 12, 570 (1957).
[11]K. Binder, in *Phase Transitions and Critical Phenomena,* edited by C. Domb and M. S. Green (Academic, London, 1976), Vol. 5b.
[12]H. De Raedt and B. De Raedt, Phys. Rev. B 18, 2039 (1978).